Role of Electronic Correlation in the Si(100) Reconstruction: A Quantum Monte Carlo Study

Sorcha B. Healy,[1] Claudia Filippi,[1] P. Kratzer,[2] E. Penev,[2] and M. Scheffler[2]

[1]*Physics Department, National University of Ireland, Cork, Ireland*

[2]*Fritz-Haber-Institut der Max-Planck-Gesellschaft, Faradayweg 4-6, D-14195 Berlin-Dahlem, Germany*

(Received 21 February 2001; published 19 June 2001)

Recent low-temperature scanning tunneling experiments have questioned the generally accepted picture of buckled silicon dimers as the ground state reconstruction of the Si(100) surface, undermining the ability of density functional theory to accurately describe electronic correlations at surfaces. We present quantum Monte Carlo calculations on large cluster models of the surface, and conclude that buckling remains energetically favorable even when the present-day best treatment of electronic correlation is employed. The implications for experimental interpretation are discussed.

DOI: 10.1103/PhysRevLett.87.016105 PACS numbers: 68.35.Bs, 71.15.–m

Despite extensive experimental and theoretical investigation, the nature of the reconstruction of the Si(100) surface is still subject to debate. While this surface is of technological relevance because of its use in the fabrication of electronic devices, determining its ground state structure is important as a test of our general understanding of the role of electronic correlation at surfaces.

Scanning tunneling microscopy (STM) experiments indicate that Si(100) reconstructs in rows of silicon dimers [1]. At room temperature, most dimers appear symmetric due to their dynamical flipping motion, and only dimers close to defects are pinned in a buckled configuration [2]. The number of symmetric dimers decreases below 120 K and dimers buckle alternately within each row, with the formation of $p(2 \times 2)$ or $c(4 \times 2)$ domains corresponding to adjacent rows in identical or opposite orientations [2,3]. Experimentally, the $c(4 \times 2)$ reconstruction (Fig. 1) was accepted as the lowest energy structure.

This picture is now being challenged by new experimental work. A series of low temperature STM studies have recently reported that, while the $c(4 \times 2)$ structure is observed below 120 K, further cooling below 20 K causes the dimers to appear again symmetric. Yokoyama and Takayanagi [4] argue that this is a dynamical phenomenon caused by a lowering of the potential energy barrier between the two buckled configurations, which allows the dimers to resume the flip-flop motion characteristic of room temperature. In contrast, Kondo *et al.* [5] claim that the observed symmetric dimers are static since their images do not exhibit the noise associated with the flipping motion observed in the same sample at 110 K. However, evidence has also been produced that, at low temperatures, the rate of dimer flipping is significantly affected by the amount of tunneling current [6], casting doubts on the conclusions drawn by Kondo *et al.* Whether the symmetric dimers are dynamic will depend on buckling being energetically favorable, and on the size of the barrier between the two buckled configurations [7].

Until now, theoretical work also remains divided on the issue. Density functional theory (DFT) calculations on slab geometries [8,9] and large cluster models [10,11] favor a buckled reconstruction. *GW* calculations [12,13] on buckled geometries show good agreement with the measured dispersion of surface band states [14], and also a surface core-level shift analysis [15] supports the DFT finding. On the other hand, multiconfiguration self-consistent field (MCSCF) and configuration interaction (CI) [16–19] calculations on small clusters find the symmetric reconstruction to have the lowest energy. These quantum chemistry techniques emphasize different components of electronic correlation than DFT: static correlation, arising from near-degeneracy of molecular orbitals, is most effectively described by a linear combination of low-lying determinants as in a MCSCF calculation, while dynamical correlation, given by short-range electronic screening, is adequately treated in DFT.

The buckling of the Si dimers on the Si(100) surface is one of the hard problems of many-body physics at surfaces, because it involves subtle aspects of electronic correlation [20]. Since the symmetric surface dimer has two dangling bonds, each filled with one electron, it is in a biradical state, and *static* correlation must be properly taken into account. The buckled state, on the other hand, is thought to be stabilized by a rehybridization of the dangling orbitals, accompanied by charge transfer: the lower Si atom approaches sp^2-like hybridization and its charge is depleted in favor of the higher Si atom in the dimer. Thus, the net stability of the buckled configuration depends on the degree to which the repulsive Coulomb interaction of the two electrons in the upper Si electronic state is dynamically screened. This is where *dynamical* correlation enters into the problem.

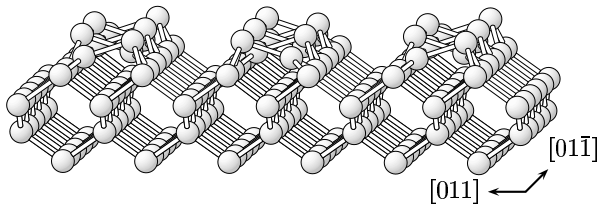

FIG. 1. Model of the silicon (100) surface in the $c(4 \times 2)$ reconstruction.

 0031-9007/01/87(1)/016105(4)$15.00

In this Letter, we use quantum Monte Carlo (QMC) methods to find accurate energy differences between the symmetric and buckled reconstructions for large cluster models of the surface. Unlike the other theoretical methods previously used for this problem, QMC has the advantage that it can be applied to sufficiently large systems and still provide an accurate description of both dynamical *and* static electronic correlation [21]. We find that dimer-dimer interactions are important and sufficiently large clusters must be used to adequately model the Si(100) surface. Our many-body calculations conclusively show that the ground state of the Si(100) surface is a buckled reconstruction, and that the trend with respect to cluster size found in DFT calculations is correct.

Cluster models of Si(100).—While methods based on DFT are known to usually give a good description of structural and elastic properties (e.g., surface lattice constant and elastic interaction between the Si dimers), it is unclear whether they can adequately represent the subtle aspects of electronic correlation at the Si(100) surface. It is therefore appropriate to use QMC on geometries obtained from DFT calculations to assess whether a more accurate treatment of electronic correlation can fundamentally change the picture. Here, we choose to address this issue by performing calculations for clusters that mimic the surface geometry.

In identifying appropriate cluster shapes for Si(100), one must recognize that interactions are negligible between neighboring dimer rows, while they are substantial between dimers in the same row. This is apparent from the small and the large dispersion of the surface band states along the respective directions, $\Gamma - J$ and $\Gamma - J'$ [13]. Moreover, the $p(2 \times 2)$ and $c(4 \times 2)$ reconstructions are found energetically quite close in experiments and calculations [9] (within 2 meV), demonstrating that dimer rows are weakly interacting.

Therefore, the surface can be modeled with clusters containing only a single row of dimers. Such clusters with one, two, and three dimers are Si_9H_{12}, $Si_{15}H_{16}$, and $Si_{21}H_{20}$, previously also used in Refs. [10,11,16–19]. They represent a four layer cut of the Si(100) surface with all but the surface atoms terminated with hydrogens to passivate dangling bonds. In Fig. 2, we show both the buckled and symmetric $Si_{15}H_{16}$ and $Si_{21}H_{20}$ clusters.

Most CI calculations have been performed on the smallest cluster Si_9H_{12} which is found to be symmetric [16,18]. Also for the $Si_{15}H_{16}$ cluster, Paulus [17] claims a symmetric ground state but the level of the CI calculation is not specified.

The Si_9H_{12} cluster is, however, too small to draw conclusions on the real surface, as became clear from recent DFT calculations [10]. For Si_9H_{12}, approximate density functionals yield conclusions similar to CI, in that buckling is either energetically unfavorable or marginally preferred by less than 4 meV. However, as the number of dimers in the cluster increases, buckling becomes favorable and the optimal buckling angle increases for all the functionals. For the three-dimer cluster $Si_{21}H_{20}$, the energy gain per dimer is between 0.15–0.20 eV, depending on the functional used, and in agreement with the slab results to better than 0.05 eV. This suggests that it is possible to infer the behavior of the Si(100) surface from the three-dimer cluster.

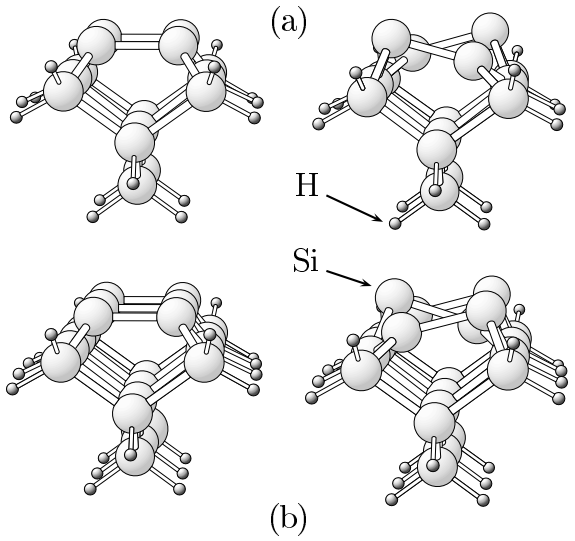

FIG. 2. $Si_{15}H_{16}$ (a) and $Si_{21}H_{20}$ (b) cluster models of the Si(100) surface. Both the symmetric (left) and buckled (right) reconstructions are shown.

Here, we perform QMC calculations on the clusters with two and three dimers, $Si_{15}H_{16}$ and $Si_{21}H_{20}$. For both clusters, we use the geometries optimized within DFT using the PW91 functional [22]. For details on the construction and the geometry of the clusters, see Ref. [10].

Silicon pseudopotential.—For the silicon atom, we use a norm-conserving sp-non-local pseudopotential for the ten core electrons. The pseudopotential was generated in an all-electron Hartree-Fock calculation for the Si atom. It was tested in QMC to calculate binding energy and bond length of Si_2, which were found in excellent agreement with experiments, and its transferability with respect to all electron calculations was checked with Hartree-Fock (HF) and B3LYP [23] for larger silicon clusters.

Quantum Monte Carlo methods.—The form of the many-body wave function used in QMC calculations efficiently describes the static part of electronic correlation by the use of a linear combination of Slater determinants, as well as its dynamical component by introducing a positive Jastrow correlation factor J (modified from Ref. [24] to deal with pseudoatoms):

$$\Psi = \sum_n d_n D_n^{\uparrow} D_n^{\downarrow} \prod_{\alpha ij} J(r_{ij}, r_{i\alpha}, r_{j\alpha}) .$$

$D_n^{\uparrow}$ and $D_n^{\downarrow}$ are Slater determinants of single particle orbitals for the up and down electrons, respectively, and the orbitals are represented using an atomic Gaussian basis [25]. The Jastrow factor correlates pairs of electrons i and

j with each other, and with every nucleus α, and different Jastrow factors are used to describe the correlation with a hydrogen and a silicon atom.

The determinantal part of the wave function is generated within HF or MCSCF, using the quantum chemistry package GAMESS [26]. As active orbitals in the MCSCF, we choose the occupied bonding and the unoccupied antibonding π orbitals, which are shown for the $Si_{15}H_{16}$ symmetric cluster in Fig. 3.

Once the determinantal part of the wave function has been determined, the parameters in the Jastrow factor are optimized within QMC using the variance minimization method [27], and the accuracy of the wave function is tested using variational Monte Carlo (VMC). Reoptimizing the determinantal part of the wave function [28] in the presence of the Jastrow factor did not lead to a significant improvement in the energy. The wave function is then used in diffusion Monte Carlo (DMC), which produces the best energy within the fixed-node approximation (i.e., the lowest-energy state with the same nodes as the trial wave function) [29]. The DMC time steps for $Si_{15}H_{16}$ and $Si_{21}H_{20}$ are 0.125 and 0.1 H^{-1}, respectively.

Results and conclusions.—Since the interplay between static and dynamical correlations is central to this problem, we first investigate the importance of accounting for near-degenerate molecular orbitals in the two-dimer clusters. For the symmetric geometry, the inclusion of determinants corresponding to the active π orbitals (Fig. 3) yields a better wave function, with a VMC energy which is 0.34 ± 0.06 eV per dimer lower than the single-determinant energy. However, within DMC, single- and multideterminant wave functions yield energies which differ only by 0.04 ± 0.02 eV per dimer. Since the DMC energy of the symmetric reconstruction is rather insensitive to the use of more than one determinant, it is not surprising that, for the buckled geometry, no energy gain is obtained either in VMC or in DMC by using a multideterminant wave function: the larger gap between the highest occupied and lowest occupied molecular orbitals (HOMO and LUMO) of the buckled cluster makes a single determinant the best option also at the variational level.

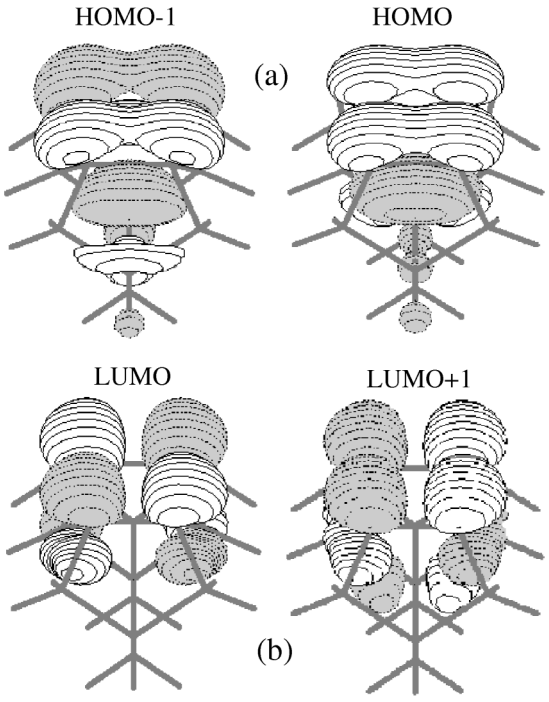

FIG. 3. Bonding (a) and antibonding (b) π orbitals for the symmetric $Si_{15}H_{16}$. The orbitals can be bonding (right) or antibonding (left) between adjacent dimers.

Since a multideterminant treatment fails to yield a significant energy gain for the two-dimer cluster, the calculations for the $Si_{21}H_{20}$ cluster are performed with one determinant only. In Table I, we list the QMC results obtained for the two- and three-dimer clusters using a single-determinant wave function.

For $Si_{15}H_{16}$, the symmetric and buckled reconstructions are energetically very close as in the case of the one-dimer cluster. With a DMC energy difference per dimer of 0.03 ± 0.02 eV, we cannot establish which reconstruction is more favorable for this cluster size. However, for $Si_{21}H_{20}$, the DMC energy gain per dimer in favor of buckling increases substantially to 0.11 ± 0.02 eV. This is in good agreement with the trends established within DFT that a one- or a two-dimer cluster fails to model the surface accurately [10].

In Fig. 4, we summarize the energy differences between the symmetric and the buckled reconstruction obtained within the local-density approximation (LDA), several generalized gradient approximations (GGA), B3LYP, and DMC. We also include results for Si_9H_{12} and the slab geometry [10]. DFT functionals predict that the buckled cluster is favored by 0.07–0.13 and 0.15–0.20 eV per dimer for $Si_{15}H_{16}$ and $Si_{21}H_{20}$, respectively. Even though the DMC energy differences are noticeably smaller than in DFT, they clearly indicate that buckling is energetically more favorable. The DMC results also highlight the importance of dimer-dimer interactions: $Si_{15}H_{16}$ behaves still very much like the single-dimer cluster and a $Si_{21}H_{20}$ cluster is needed to be able to resolve the energy gain in favor of the buckled geometry. For larger clusters, we expect an increase in the DMC gain for buckling, as seen

TABLE I. VMC and DMC energy differences between the symmetric (E_{sym}) and buckled (E_{buck}) reconstructions of the $Si_{15}H_{16}$ and $Si_{21}H_{20}$ clusters. $\Delta E = E_{sym} - E_{buck}$ and the numbers in parentheses are the statistical errors on the last two figures. Energies are in eV.

		ΔE	ΔE/dimer
$Si_{15}H_{16}$	VMC	0.53(13)	0.27(06)
	DMC	0.06(04)	0.03(02)
$Si_{21}H_{20}$	VMC	0.70(14)	0.23(05)
	DMC	0.34(06)	0.11(02)

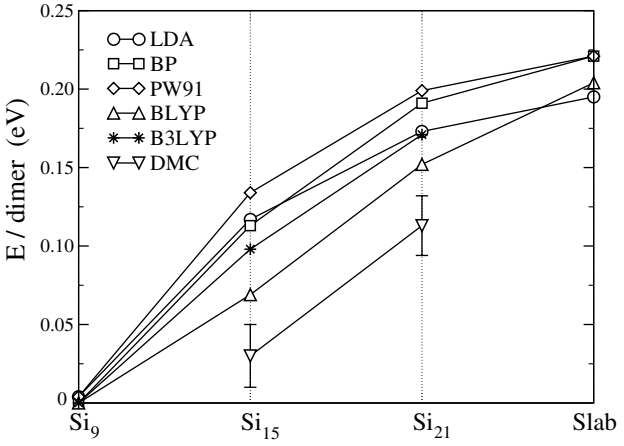

FIG. 4. Energy differences per dimer for the symmetric and buckled reconstructions ($\Delta E = E_{\text{sym}} - E_{\text{buck}}$) obtained with LDA, various GGA functionals, and DMC.

in the DFT calculations: the electronic states become more extended, and DFT will predict the correct trend when going from an already large cluster to the surface.

In this Letter, we presented accurate QMC calculations of the energies of the buckled and symmetric reconstruction of the Si(100) surface, and determined that the buckled geometry is lower in energy. Our calculations show that electronic interactions between adjacent Si dimers in a row are important to obtain the buckled ground state, and large clusters must be used to adequately model the Si(100) surface. While DFT-LDA/GGA calculations tend to overestimate the energy gain due to buckling, they correctly reproduce the trend with cluster size. Having established a buckled ground state, the symmetric dimers observed in STM experiments at 6 K must be dynamically flipping. A rough extrapolation of the DMC energy gain to infinite size yields a barrier for flipping of about 0.15 eV, in good agreement with experimental estimates [7]. Such a large value rules out thermal activation as the flipping mechanism at 6 K, although quantum effects of the Si motion could be responsible for the experimental observations.

We thank C. Umrigar and S. Fahy for useful discussions, and E. Shirley for the use of his code to generate the HF pseudopotential. This work is supported by Enterprise Ireland Grant No. SC/99/242 and the Irish Higher Education Authority.

[1] R. J. Hamers, R. M. Tromp, and J. E. Demuth, Phys. Rev. B **34**, 5343 (1986).
[2] R. A. Wolkow, Phys. Rev. Lett. **68**, 2636 (1992).
[3] H. Tochihara, T. Amakusa, and M. Iwatsuki, Phys. Rev. B **50**, 12 262 (1994).
[4] T. Yokoyama and K. Takayanagi, Phys. Rev. B **61**, R5078 (2000).
[5] Y. Kondo *et al.,* Surf. Sci. **453**, L318 (2000).
[6] T. Mitsui and K. Takayanagi, Phys. Rev. B **62**, R16 251 (2000).
[7] K. Hata, Y. Sainoo, and H. Shigekawa, Phys. Rev. Lett. **86**, 3084 (2001).
[8] J. Dabrowski and M. Scheffler, Appl. Surf. Sci. **56–58**, 15 (1992).
[9] K. Inoue *et al.,* Phys. Rev. B **49**, 14 774 (1994); A. Ramstad, G. Brocks, and P. J. Kelly, *ibid.* **51**, 14 504 (1995).
[10] E. Penev, P. Kratzer, and M. Scheffler, J. Chem. Phys. **110**, 3986 (1999).
[11] R. Konecny and D. J. Doren, J. Phys. Chem. B **101**, 10 983 (1997); J. Chem. Phys. **106**, 2426 (1997); C. Yang, S. Y. Lee, and H. C. Kang, *ibid.* **107**, 3295 (1997).
[12] J. E. Northrup, Phys. Rev. B **47**, 10 032 (1993).
[13] M. Rohlfing, P. Krüger, and J. Pollmann, Phys. Rev. B **52**, 13 753 (1995).
[14] L. S. O. Johansson *et al.,* Phys. Rev. B **42**, 1305 (1990).
[15] E. Pehlke and M. Scheffler, Phys. Rev. Lett. **71**, 2338 (1993).
[16] M. R. Radeke and E. A. Carter, Phys. Rev. B **54**, 11 803 (1996).
[17] B. Paulus, Surf. Sci. **408**, 195 (1998).
[18] Z. Jing and J. L. Whitten, J. Chem. Phys. **98**, 7466 (1993).
[19] J. Shoemaker, L. W. Burggraf, and M. S. Gordon, J. Chem. Phys. **112**, 2994 (2000); J. S. Hess and D. J. Doren, *ibid.* **113**, 9353 (2000); M. S. Gordon, J. Shoemaker, and L. W. Burggraf, *ibid.* **113**, 9355 (2000).
[20] O. Paz *et al.,* Surf. Sci. (to be published).
[21] W. M. C. Foulkes *et al.,* Rev. Mod. Phys. **73**, 33 (2001), and references therein.
[22] J. P. Perdew, in *Electronic Structure of Solids '91,* edited by P. Ziesche and H. Eschrig (Akademie-Verlag, Berlin, 1991).
[23] A. D. Becke, J. Chem. Phys. **98**, 5648 (1993); C. Lee, W. Yang, and R. G. Parr, Phys. Rev. B **37**, 785 (1988).
[24] C. Filippi and C. J. Umrigar, J. Chem. Phys. **105**, 213 (1996).
[25] The Gaussian basis sets are $(10s10p1d)/[3s3p1d]$ for silicon and $(10s1p)/[3s1p]$ for hydrogen, and are optimized at the HF level for the Si_9H_{12} cluster.
[26] M. W. Schmidt *et al.,* J. Comput. Chem. **14**, 1347 (1993).
[27] C. J. Umrigar, K. G. Wilson, and J. W. Wilkins, Phys. Rev. Lett. **60**, 1719 (1988).
[28] C. Filippi and S. Fahy, J. Chem. Phys. **112**, 3523 (2000).
[29] P. J. Reynolds *et al.,* J. Chem. Phys. **77**, 5593 (1982); L. Mitas, E. L. Shirley, and D. M. Ceperley, *ibid.* **95**, 3467 (1991); C. J. Umrigar, M. P. Nightingale, and K. J. Runge, *ibid.* **99**, 2865 (1993).